3D DC resistivity modeling of steel casing for reservoir monitoring using equivalent resistor network

Dikun Yang, Douglas W. Oldenburg, and Lindsey J. Heagy, Geophysical Inversion Facility, University of British Columbia*

SUMMARY

Energized steel casings in oilfields channel electric currents generated for a surface resistivity survey down to the depth of target reservoir, enabling the use of electric methods in reservoir monitoring. Numerical simulation of such a survey often requires refined meshes to simulate the casing. In order to avoid the use of small cells, we propose a method that treats the earth's conductivity model as a 3D equivalent resistor network (ResNet), and a casing as a parallel-circuit wire conductor. Numerical comparisons with a cylindrically symmetric code and with a finite element code show that ResNet provides accurate and efficient solutions to the current along the casing and to the electric field on the surface. Using ResNet, we further study how the current distributes along a casing: (1) The casing current approaches a nearly linear decay if the casing conductivity is sufficiently high; (2) The casing current is more sensitive to variation in the extent of a conductive injectate than that of a resistive one; (3) Under special circumstances the current can flow into the casing from the surrounding.

INTRODUCTION

Metallic (steel) casing is common in oilfield settings. Due to its extremely high conductivity and elongated geometry, casing has been an interesting subject in DC/EM for decades. It was once considered a source of interference in regular DC/EM surveys (Holladay and West, 1984; Schenkel and Morrison, 1990). Then it was treated within the context of borehole electric surveys, in which the resistivity of the adjacent formation is of interest (Schenkel and Morrison, 1994). A steel casing can also be used as an extended electrode by connecting an electric source/receiver to it (Rocroi and Koulikov, 1985; Rucker et al., 2010). This idea has re-gained attention recently for its potential of being used in the monitoring of fluid injection (e.g. in hydraulic fracturing and CO_2 sequestration). The benefit of energizing a casing to detect the conductivity change in the reservoir can be understood in two ways: (1) Casing can channel the current down to greater depth, causing extra charges to build up on deep conductivity interfaces that boost the anomalous electric field (E-field) signals; (2) Treated as an equipotential object, a casing effectively reduces the "resistance distance" between the sources/receivers on the surface and the injected materials, so the surface measurement can reflect the subtle changes at depth.

Different approaches have been developed to numerically model the effect of casing. The casing system (casing wall, well fluid and the surrounding formation) can be approximated by a transmission-line model and solved on an equivalent RLC circuit (Kaufman, 1990; Aldridge et al., 2015). For realistic problems at reservoir-scale, the casing is usually handled using cells much smaller than those necessary to capture the surrounding geology. One straightforward approach is to model the entire casing system with cells a fraction of the casing thickness (Commer et al., 2015; Hoversten et al., 2015). It provides the most complete solution of the casing system, but requires significant computing resources. By assuming the casing system is cylindrically symmetric, the casing problem can have a reduced form, saving computing time (Schenkel and Morrison, 1990; Heagy et al., 2015). Another more economical approach is upscaling, which calculates the effective conductivity of the cells containing the casing (Rucker et al., 2010; Caudillo-Mata et al., 2014; Weiss et al., 2015). Although upscaling is a reasonable trade-off between the accuracy and the cost, it still often requires casing cells much smaller than regular earth cells to approximate the casing. The fastest solution is provided by Daily et al. (2004), which does not require smaller-than-usual cells. It first computes the conductances on the edges of a finite difference 3D mesh, then alters the conductances where the casing exists, according to the casing conductivity and cross section.

In our study, we generalize Daily's approach with the help of equivalent resistor network (ResNet). This reformulation allows us to handle all types of highly anisotropic objects without any refinement of the mesh. Our approach does not model the fine-scale casing system, but the approximation is accurate enough if the scale of investigation is much greater than the diameter of casing. We focus only on DC source, but the distribution of casing current can provide insights for EM.

METHODOLOGY

ResNet solves the DC modeling problem in two steps: (1) Transform the actual continuous medium model to an equivalent resistor network; (2) Solve the circuit problem using Kirchhoff's laws. For simplicity, we assume that a 3D rectangular mesh is used to describe the earth's conductivity model and the well path. In ResNet, conducting objects can be represented using three types of (pseudo-) conductivity that are eventually transformed to equivalent resistors:

(1) *Cell conductivity*: defined at cell centers for 3D volumic objects. This is used to describe arbitrarily shaped geologic objects the same way as in the regular DC/EM algorithms. Cell conductivity is the intrinsic conductivity (σ_c in S/m).

(2) *Face pseudo-conductivity*: defined on cell faces for 2D sheet objects, like thin layers of sediment or fractures, where one of the three dimensions vanishes. Face pseudo-conductivity is the product of its intrinsic conductivity and the thickness ($\hat{\sigma}_f = \sigma_c \cdot h$ in S).

(3) *Edge pseudo-conductivity*: defined on mesh edges for 1D line objects that are elongated in one direction, like casing underground or pipeline on surface. Edge pseudo-conductivity is the product of its intrinsic conductivity and the cross section area ($\hat{\sigma}_e = \sigma_c \cdot w \cdot h$ in S·m).

An equivalent resistor network circuit can be constructed directly using the 3D mesh: the mesh nodes are treated as junctions, and the edges as branches. ResNet requires the three types of (pseudo-) conductivity to collapse into conductances defined on edges. By definition, the directional conductance G of a conductor with uniform cross section is

$$G = \frac{wh\sigma_c}{\ell}, \tag{1}$$

where σ_c is the intrinsic conductivity, and w, h, ℓ are respectively the width, height and length of the object. An edge has four neighboring cells, so the edge conductance also contains contributions from those four cells in parallel (Figure 1a). While the conductivity σ_c and the edge length ℓ are known, the cross section $(w \cdot h)$ of each of the four conductors can be calculated using the conductor's volume, which is one fourth of the total volume of the cell it belongs to. Using equation 1, the conductance from one neighboring cell is calculated by

$$G_c = \frac{V}{4\ell} \cdot \frac{\sigma_c}{\ell}, \tag{2}$$

where $V = w \cdot h \cdot \ell$ is the volume of the corresponding cell. Then the total conductance on an edge from the cell conductivity is the sum of the four conductors. Similarly, an edge has four neighboring faces, and the conductance from one of the faces is

$$G_f = \frac{A}{2\ell} \cdot \frac{\hat{\sigma}_f}{\ell}, \tag{3}$$

where $A = w \cdot \ell$ is the area of the corresponding face (Figure 1b). Finally an edge pseudo-conductivity also contributes to the edge conductance according to

$$G_e = \frac{\hat{\sigma}_e}{\ell}. \tag{4}$$

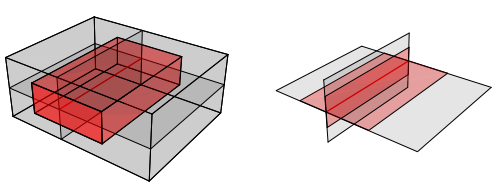

(a) (b)

Figure 1: Cell conductivity (a) and face pseudo-conductivity (b) collapse to a conductance on the red edge.

Organizing σ_c, $\hat{\sigma}_f$ and $\hat{\sigma}_e$ as model vectors, the total conductance assigned to the resistor on each branch of the circuit is the conductances from G_c, G_f, and G_e summed in parallel:

$$\mathbf{g} = \mathbf{A}_c\sigma_c + \mathbf{A}_f\hat{\sigma}_f + \mathbf{A}_e\hat{\sigma}_e, \tag{5}$$

where $\mathbf{A}_c$, $\mathbf{A}_f$ and $\mathbf{A}_e$ represent the calculation in equation 2 to 4. Fluid within the well bore, if necessary, can be added to equation 5 as another $\mathbf{A}_e\hat{\sigma}_e$ term. The transformation of a model on a 3D mesh to its equivalent resistor network is illustrated in Figure 2.

After the derivation of an equivalent circuit, simulating a DC survey is equivalent to connecting current sources to some junctions of the circuit, and measuring the potential difference between two junctions. ResNet defines the potential ϕ on junctions, then the potential difference across a branch can be computed using a differential matrix $\mathbf{D}$. The current flowing along

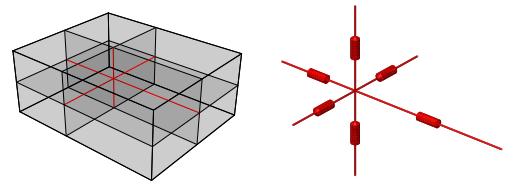

(a) (b)

Figure 2: Part of a 3D mesh (a) and its local equivalent resistor network (b). The six red edges in the mesh are transformed to branches of a circuit built with equivalent resistors calculated using cell, face and edge (pseudo-)conductivities.

a branch is the product of the potential difference and the conductance. Finally, using Kirchhoff's current law, the linear system of the forward modeling is

$$-\mathbf{D}^\top\mathbf{G}\mathbf{D}\phi = \mathbf{s}, \tag{6}$$

where $\mathbf{G}$ is a diagonal matrix of vector $\mathbf{g}$ in equation 5, $\mathbf{s}$ indicates where the current source is connected to the circuit. Equation 6 has apparence similar to the $\nabla \cdot \sigma \nabla$ equation used in most DC codes, but there is meaningful difference. In regular DC codes, the geometric information about the mesh is embedded in the gradient and divergence matrix (normalized $\mathbf{D}$), so only cell conductivity can be modeled. ResNet incorporates the mesh information into the conductance term to allow the modeling of thin objects by using face and edge pseudo-conductivities. The formulation of an equivalent circuit implicitly uses a no-flux boundary condition.

TEST AGAINST CYLINDRICALLY SYMMETRIC CODE

We test ResNet code using the model in FIG. 2 of Schenkel and Morrison (1990). The casing is 300 m long with center radius of 0.1 m and thickness of 0.006 m. The conductivity of the casing and the uniform background (including the well fluid) is 10^6 and 10^{-2} S/m, respectively. The current source (1 A) electrode is in direct contact with the casing wall at the depth of 300 m. The return current electrode is placed at infinity.

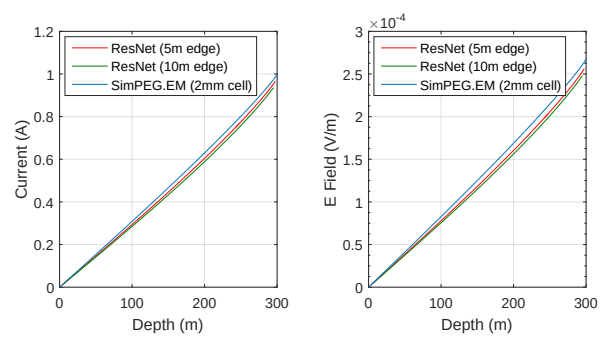

(a) (b)

Figure 3: Comparison between a cylindrically symmetric code and ResNet based on a vertical casing and a down-hole source in a half-space: (a) Current and (b) E-field along the casing.

The complete casing system is modeled using SimPEG.EM,

a cylindrically symmetric 2D finite volume EM code (Heagy et al., 2015; Cockett et al., 2015). The casing's wall is modeled by 3 cells, each 2 mm thick, and the CPU time is about 30 s on a desktop computer. The script is available online via Figshare (Heagy, 2016).

In ResNet, the edge pseudo-conductivity of the casing and the well fluid are calculated to be 3770 S·m and 2.8×10^{-4} S·m, respectively. Two simulations using 10 m and 5 m edge lengths are tested, and their CPU times are 4.4 s and 16 s respectively. The 5 m edge length offers better approximation near the source (Figure 3). ResNet's accuracy can be improved by locally using shorter edges around the source. This example demonstrates that ResNet can reasonably simulate the current and E-field along the casing without using very small cells.

TEST AGAINST FINITE ELEMENT METHOD

Next we compare ResNet with published finite element method (FEM) using conductivity upscaling approach. We adopt the hydraulic fracturing model in Weiss et al. (2015), and examine the E-field measurement on the surface. The earth consists of three layers: 0.001 S/m from the surface to 300 m depth, 0.0002 S/m from 300 m to 800 m depth , and 0.03 S/m below 800 m. The vertical section of the well goes from the surface to a depth of 2360 m, and then turns horizontally along Y direction (from Y = 0 to 1570 m). The DC sources are connected to the wellhead and on the surface at Y = -1000 m. The fractured region consists of four parallel slabs with a conductivity 10 S/m at the well-heel, each of which is $5 \times 60 \times 100$ m in size, and 15 m apart from each other. Weiss et al. (2015) modeled the casing as a column of conductive cells (effective radius 10 m) on an tetrahedral mesh with local refinement around the casing; the casing cells are assigned a volume-averaged conductivity of 10^4 S/m. A 100 m dipole array measurement is simulated on the surface in line with the well path to examine whether the difference in E-field between pre- and post-fracturing is detectable.

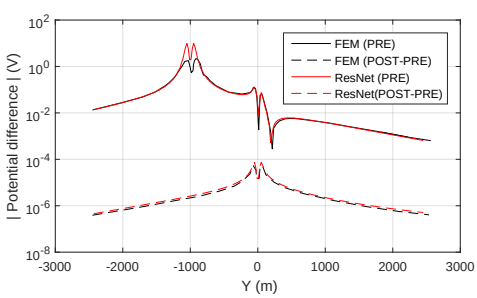

Figure 4: Surface measurements of a fracturing model simulated using ResNet and finite element method.

ResNet models the same scenario using an edge length of 50 m. The edge pseudo-conductivity of the casing is 3.14×10^6 S·m. The fracture slabs are treated as a face conductivity of 200 S perpendicular to the horizontal well. Both pre- and post-fracturing are simulated, and each takes about 10 seconds. The results obtained by ResNet are largely similar to those by FEM for both the baseline (PRE) and the anomalous field (POST-PRE) (Figure 4). Discrepancy is observed at the surface source (Y = -1000 m), but not at the wellhead (Y = 0 m). This implies that the singularity of a surface source requires shorter edge length around it, while a casing that diffuses the source intensity is more tolerant of a long edge length.

CALCULATING CASING CURRENTS

One of the applications of ResNet is to calculate casing current for an arbitrary 3D model. The casing current can be used to derive the current leakage into the formation along the well path. Then the casing can be approximated by a distributed current source. Those equivalent sources dominate the first-order effect in the data measured on the surface. By implementing them in a DC inversion code, the DC data from a casing survey can be inverted without modeling the casing.

Impact of casing conductivity

The effectiveness of delivering current to depth largely depends on the casing's conductivity. We use the vertical casing model in a 10^{-2} S/m half-space in the first test, but explore different casing conductivities. The current source of 1 A is moved from the end of well to the wellhead on the surface. We have found that if the conductivity ratio between the casing and the surrounding is high enough, the casing current approaches a nearly linear decay, implying a more uniform distribution of equivalent sources along the casing. If the casing conductivity continues to decline, the distribution of current will behave more like in the case of a point source on the surface of a uniform half-space (Figure 5).

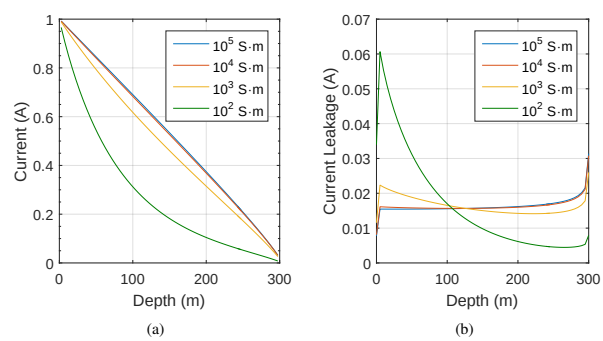

Figure 5: Casing of different edge pseudo-conductivities: (a) Total current and (b) current leakage along the casing.

Injection

We investigate how the casing current responds to the injection of fluid into the reservoir. We use a conductive injectate to represent a fracture operation, and a resistive injectate for CO_2 sequestration. The casing conductivity is set to be high enough that the casing current decays linearly if no fluid is injected. The conductive injectate is a 1 m thick slab of 1 S/m at the depth of 200 m penetrated by the casing at the center; the lateral extent of the slab can be large or small (Figure 6). The resistive injectate has the same lateral variation, but is a 20 m thick block (Z = -190 to -210 m) of 10^{-3} S/m. The conductive

slab is modeled with an equivalent face pseudo-conductivity in ResNet, and the resistive block in its actual size and with cell conductivity.

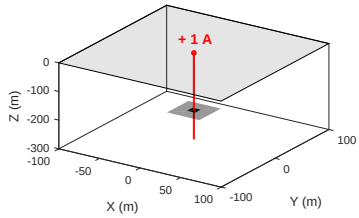

Figure 6: Injection model with a variable lateral extent of 40 × 40 m (grey) or 10 × 10 m (black).

Using the half-space as a reference, the conductive body creates a sharp drop at the depth of 200 m on the curve of casing current (Figure 7a), because the injected fluid serves as an easy escape of the current (Figure 7b). In contrast, for a resistive block, the curve of casing current is flat at the depth of injection (Figure 8a), because a resistive surrounding prevents the current from leaking out of the casing (Figure 8b).

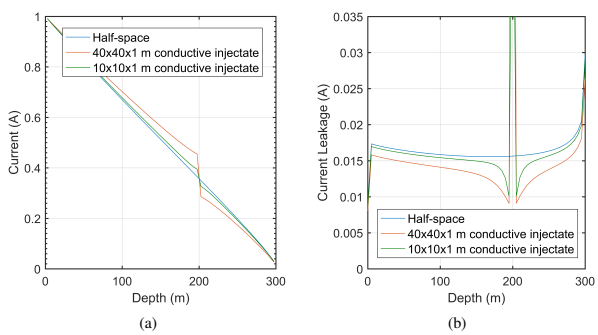

Figure 7: Injecting a conductive slab of variable lateral extent: (a) Total current and (b) current leakage along the casing.

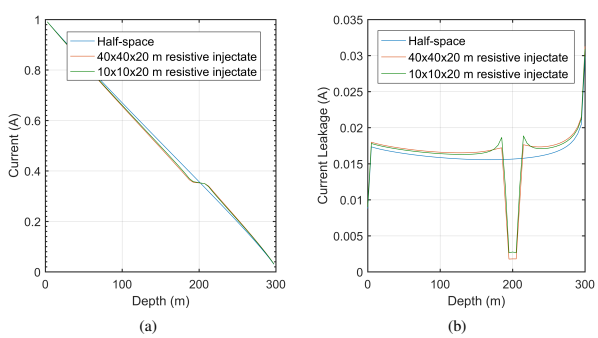

Figure 8: Injecting a resistive block of variable lateral extent: (a) Total current and (b) current leakage along the casing.

In both cases, the current leakage responds to the size of the injection, suggesting the possibility of inferring the geometry of injection from surface data. However, the variation of the injection's extent is more pronounced in the conductive case than in the resistive case. Quantifying the lateral extent of medium that the casing current is sensitive to, we conclude that a conductive surrounding has a greater "radius of sensitivity" than does a more resistive one. This can make the delineation of a resistive injectate more difficult.

Negative leakage

Intuition suggests that the current always flows out of a casing, because the casing conductivity is always much greater than that of the earth medium. However, it is possible for the current to flow from the formation to the casing under certain circumstances. We show this using an example based on the same 300 m casing model, but the edge pseudo-conductivity of the casing is 10 S·m, and a resistive layer of 10^{-4} S/m is added to Z = -250 to -260 m. Above a depth of 200 m, current leaks off from the casing in a manner similar to a uniform half-space (Figure 9a), but near the resistive layer, we see that direction of the current reverses as current is directed towards the casing at X = 0 m (Figure 9b).

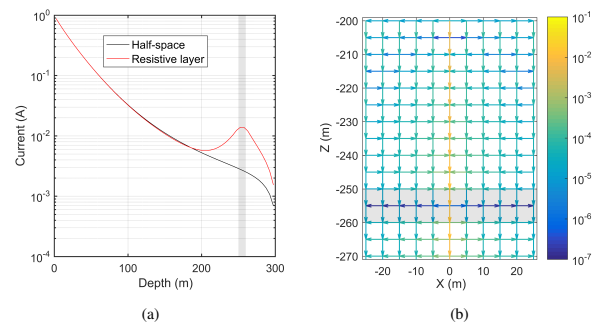

Figure 9: Currents flowing from the formation to the casing: (a) Total current along the casing; (b) Cross section view of currents around the casing on the edges of the resistor network (color in A). The resistive layer is marked by the shaded area.

A sufficiently conductive casing only creates horizontal current flow in close vicinity of the casing, but Figure 9b reveals that significant down-going currents exist as a result of low casing conductivity and/or deep casing. A resistive layer can block the down-going currents and force them to seek alternaive routes. A casing that short-cuts the resistive barrier then becomes a funnel gathering the previously leaked current.

CONCLUSION

Many approaches have been proposed to model the casing's effect in a DC/EM survey, but they either require cylindrical symmetry or very small cells. We propose an approach (ResNet) for DC that transforms the earth's conductivity model to an equivalent circuit. This equivalent circuit allows us to model thin objects (e.g. casing, pipeline, thin fractures, etc.) by adding parallel-circuit conductance to the resistor network; so the number of variables for solve is still the same as in a no-casing modeling. ResNet is satisfactorily tested against a cylindrically symmetric code for casing current, and a finite element solution for surface measurement. Although ResNet does not compute the details inside the casing, it offers a fast solution at the scale most borehole-surface surveys take place.

EDITED REFERENCES

Note: This reference list is a copyedited version of the reference list submitted by the author. Reference lists for the 2016 SEG Technical Program Expanded Abstracts have been copyedited so that references provided with the online metadata for each paper will achieve a high degree of linking to cited sources that appear on the Web.

REFERENCES

Aldridge, D. F., C. J. Weiss, H. A. Knox, K. A. Schramm, and L. C. Bartel, 2015, Is a steel-cased borehole an electrical transmission line?: 85th Annual International Meeting, SEG, Expanded Abstracts, 736–741, http://dx.doi.org/10.1190/segam2015-5927874.1.

Caudillo-Mata, L., E. Haber, L. Heagy, and D. Oldenburg, 2014, Numerical upscaling of electrical conductivity: A problem specific approach to generate coarse-scale models: 84th Annual International Meeting, SEG, Expanded Abstracts, 680–684, http://dx.doi.org/10.1190/segam2014-1488.1.

Cockett, R., S. Kang, L. J. Heagy, A. Pidlisecky, and D. W. Oldenburg, 2015, SimPEG: An open source framework for simulation and gradient based parameter estimation in geophysical applications: Computers & Geosciences, **85**, 142–154, http://dx.doi.org/10.1016/j.cageo.2015.09.015.

Commer, M., G. M. Hoversten, and E. S. Um, 2015, Transient electromagnetic finite-difference time-domain earth modeling over steel infrastructure: Geophysics, **80**, no. 2, E147–E162, http://dx.doi.org/10.1190/geo2014-0324.1.

Daily, W., A. Ramirez, R. Newmark, and K. Masica, 2004, Low-cost reservoir tomographs of electrical resistivity: The Leading Edge, **23**,, 472–480, http://dx.doi.org/10.1190/1.1756837.

Heagy, L., 2016, SimPEG.EM casing example based on the Schenkel and Morrison casing model, https://dx.doi.org/10.6084/m9.figshare.3126961.v1, accessed 31 March 2016.

Heagy, L. J., R. Cockett, D. W. Oldenburg, and M. Wilt, 2015, Modelling electromagnetic problems in the presence of cased wells: 85th Annual International Meeting, SEG, Expanded Abstracts, 699–703, http://library.seg.org/doi/abs/10.1190/segam2015-5931035.1.

Holladay, J. S., and G. West, 1984, Effect of well casings on surface electrical surveys: Geophysics, **49**, 177–188, http://dx.doi.org/10.1190/1.1441649.

Hoversten, G. M., M. Commer, E. Haber, and C. Schwarzbach, 2015, Hydro-frac monitoring using ground time-domain electromagnetics: Geophysical Prospecting, **63**, 1508–1526, http://dx.doi.org/10.1111/1365-2478.12300.

Kaufman, A. A., 1990, The electrical field in a borehole with a casing: Geophysics, **55**, 29–38, http://dx.doi.org/10.1190/1.1442769.

Rocroi, J., and A. Koulikov, 1985, The use of vertical line sources in electrical prospecting for hydrocarbon: Geophysical Prospecting, **33**, 138–152, http://dx.doi.org/10.1111/j.1365-2478.1985.tb00426.x.

Rucker, D. F., M. H. Loke, M. T. Levitt, and G. E. Noonan, 2010, Electrical-resistivity characterization of an industrial site using long electrodes: Geophysics, **75**, no. 4, WA95–WA104, http://dx.doi.org/10.1190/1.3464806.

Schenkel, C. J., and H. F. Morrison, 1990, Effects of well casing on potential field measurements using downhole current sources: Geophysical Prospecting, **38**, 663–686, http://dx.doi.org/10.1111/j.1365-2478.1990.tb01868.x.

Schenkel, C. J., and H. F. Morrison, 1994, Electrical resistivity measurement through metal casing: Geophysics, **59**, 1072–1082, http://dx.doi.org/10.1190/1.1443663.

Weiss, C. J., D. F. Aldridge, H. A. Knox, K. A. Schramm, and L. C. Bartel, 2015, The DC response of electrically conducting fractures excited by a grounded current source: 85th Annual International Meeting, SEG, Expanded Abstracts, 930–936, http://dx.doi.org/10.1190/segam2015-5870407.1.